

Biophysical Journal, Volume 116

Supplemental Information

Identification of Binding Sites for Efflux Pump Inhibitors of the AcrAB-TolC Component AcrA

Zbigniew M. Darzynkiewicz, Adam T. Green, Narges Abdali, Anthony Hazel, Ronnie L. Fulton, Joseph Kimball, Zygmunt Gryczynski, James C. Gumbart, Jerry M. Parks, Jeremy C. Smith, and Helen I. Zgurskaya

```

AcrA/1-397 -----
MexA/1-360 -----
CusB/1-413 MKKIALIIGSMIAGGIISAAGFTWVAKAEPPEKTSTAERKILF

AcrA/1-397 ---MKNKNRGFTPLAVVLMLSGSLALTGCDDKQ---AQGGGQ
MexA/1-360 ---SGKS---EAPPPAQ
CusB/1-413 WYDPMYPNRFDKPGKSPFMDMDLVPKYADEESSASGVRIDPTQ

AcrA/1-397 MPAVG--VTVKTEPLQITTELPGRT--SAYRIAEVRPQVSGII
MexA/1-360 TPEVG--IVTLEAQTVTLNTELPGRT--NAFRIAEVRPQVNGI
CusB/1-413 TQNLGVKTATVTRGPLTFAQSFPANVSYNEYQYAIVQARAAGFI

AcrA/1-397 LKR-NFKEGSDIEAGVSLYQIDPATYQATYDSAKGDLAKAQAAA
MexA/1-360 LKR-LFKEGSDVKAGQQLYQIDPATYEADYQSAQANLASTQEQ-
CusB/1-413 DKVYPLTVGDKVQKGTPLLDLTIPDWV---EAQS-----

AcrA/1-397 NIAQLTVNRYQKLLGTQYISKQEYDQALADAQQANAAVTAAKAA
MexA/1-360 -----AQRYKLLVADQAVSKQYADA-----NAAYLQSKAA
CusB/1-413 -----EYLLLRETGGTA-TQTEGILERLRLAGMPEADIRRL

AcrA/1-397 VETARINLAYTKVTSPISGRIGKSNVTEGALVQNGQATALATVQ
MexA/1-360 VEQARINLRYTKVLSPISGRIGRSAVTEGALVTNGQANAMATVQ
CusB/1-413 IATQKIQTRF-TLKAPIDGVITAFDLRAGMNI--AKDNVVAKIQ

AcrA/1-397 QLDPIYVDVTQSSNDFLRLKQELANGTLKQEN-GKAKVSLITSD
MexA/1-360 QLDPIYVDVTQPSTALLRLRRELASGQLERAGDNAAKVSLKLED
CusB/1-413 GMDPVWVTAAIPESIAWLVK-----D

AcrA/1-397 GIKFPQ-----DGTLEF-----SDVTVDQTTGSITLRAIFPNPD
MexA/1-360 GSQYPL-----EGRLEF-----SEYSVDEGTGSVTIRAVFPNPN
CusB/1-413 ASQFTLTVPARPDKTLTIRKWTLLPGVDAAIRTLQLRLEVDNAD

AcrA/1-397 HTLLPGMFVRARLEEGLNPNAILVPQQGVTRTPRGDATVLVVGA
MexA/1-360 NELLPGMFVHAQLQEGVKQKAILAPQQGVTRDLKGQATALVVNA
CusB/1-413 EALKPGMNAWLQLNTASEPML-LIPSQALIDTGS-EQRVITVDA

AcrA/1-397 DDKVETRPIVASQAIGDKWLVTEGLKAGDRVVISGLQKVRPGVQ
MexA/1-360 QNKVELRVIKADRVIGDKWLVTEGLNAGDKIITEGLQFVQPGVE
CusB/1-413 DGRFVPKRVAVFQASQGVTALRSGLAEGEKVVSSGLFLIDSEAN

AcrA/1-397 VKAQEVTADNNQQASGAQPEQSKS--
MexA/1-360 VKTVPAKNVASAQKAD-AAPAKTDSKG
CusB/1-413 ISGALERMRSE--SATHAHHHHHHH--

```

Figure S1. Sequence alignment of full-length AcrA, MexA (chain F from PDB 2V4D) and CusB (chain C from PDB 3NE5).

The sequence of full-length wild-type AcrA (residues 1-397) is listed below. The portion of the sequence included in the homology model (residues 38-379) is shown in bold.

```

>NP_414996.1 multidrug efflux system [Escherichia coli str. K-12 substr.
MG1655]
MNKNRGFTPLAVVLMLSGSLALTGCDDKQAQGGGQMPAVGVVTVKTEPLQITTELPGRTSAYRIAEVRP
QVSGILKRNFKEGSDIEAGVSLYQIDPATYQATYDSAKGDLAKAQAAANIAQLTVNRYQKLLGTQYISK
QEYDQALADAQQANAAVTAAKAAVETARINLAYTKVTSPISGRIGKSNVTEGALVQNGQATALATVQLD
PIYVDVTQSSNDFLRLKQELANGTLKQENGKAKVSLITSDGIKFPQDGTLEFSDVTVDQTTGSITLRAI
FPNPDHTLLPGMFVRARLEEGLNPNAILVPQQGVTRTPRGDATVLVVGADDKVETRPIVASQAIGDKWLVT
EGLKAGDRVVISGLQKVRPGVQE

```

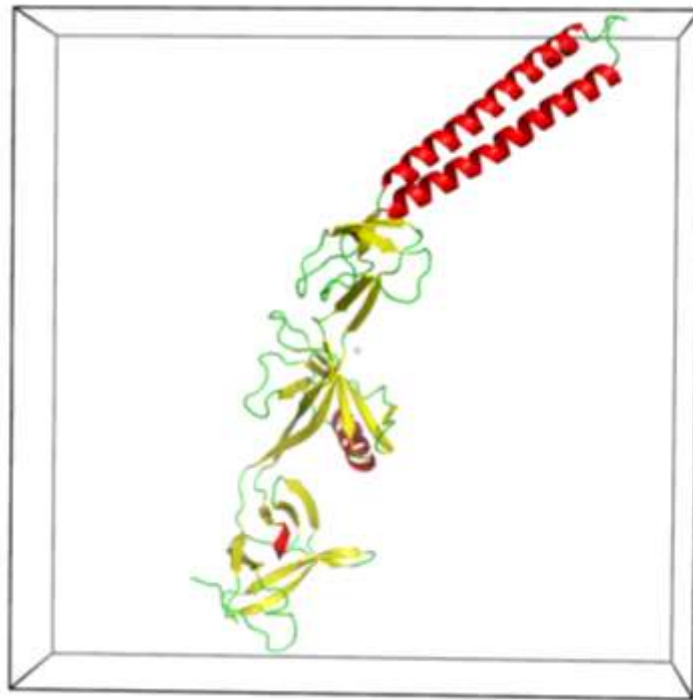


Figure S2. Search space used for docking. The dimensions of the box are 126 Å x 126 Å x 50 Å.

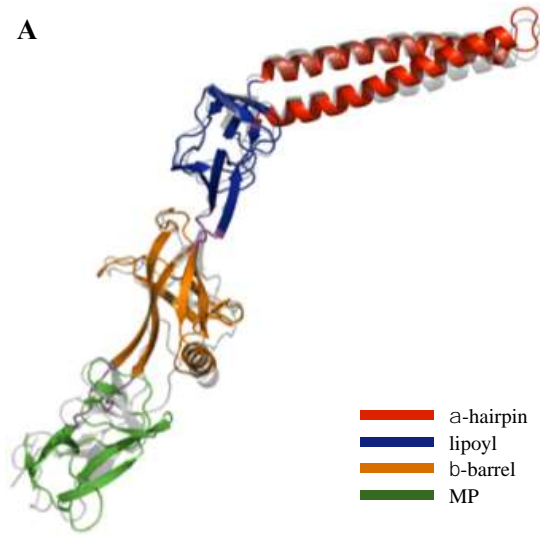
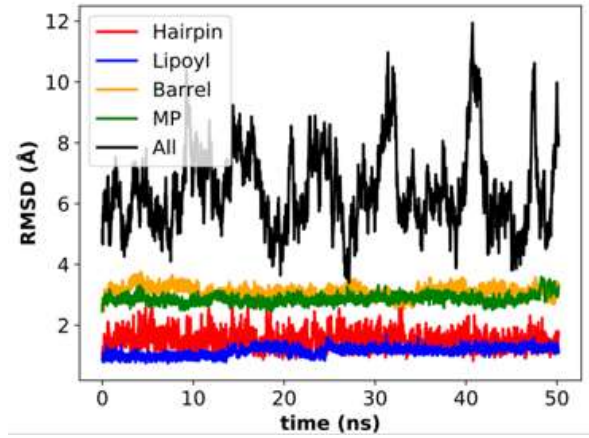
A**B**

Figure S3. (A) Superposition of the homology model of WT AcrA monomer onto an AcrA protomer from the cryo-EM structure of the assembled AcrAB-TolC complex. *Colors:* hairpin (red), lipoyl (blue), barrel (orange), and MP domain (green), chain D from PDB entry 5v5s (gray). The linkers are shown in magenta and were not included in the RMSD calculations for the individual domains. (B) C α RMSD of AcrA for the whole protein and for each individual domain with respect to the cryo-EM model over the course of the MD simulation.

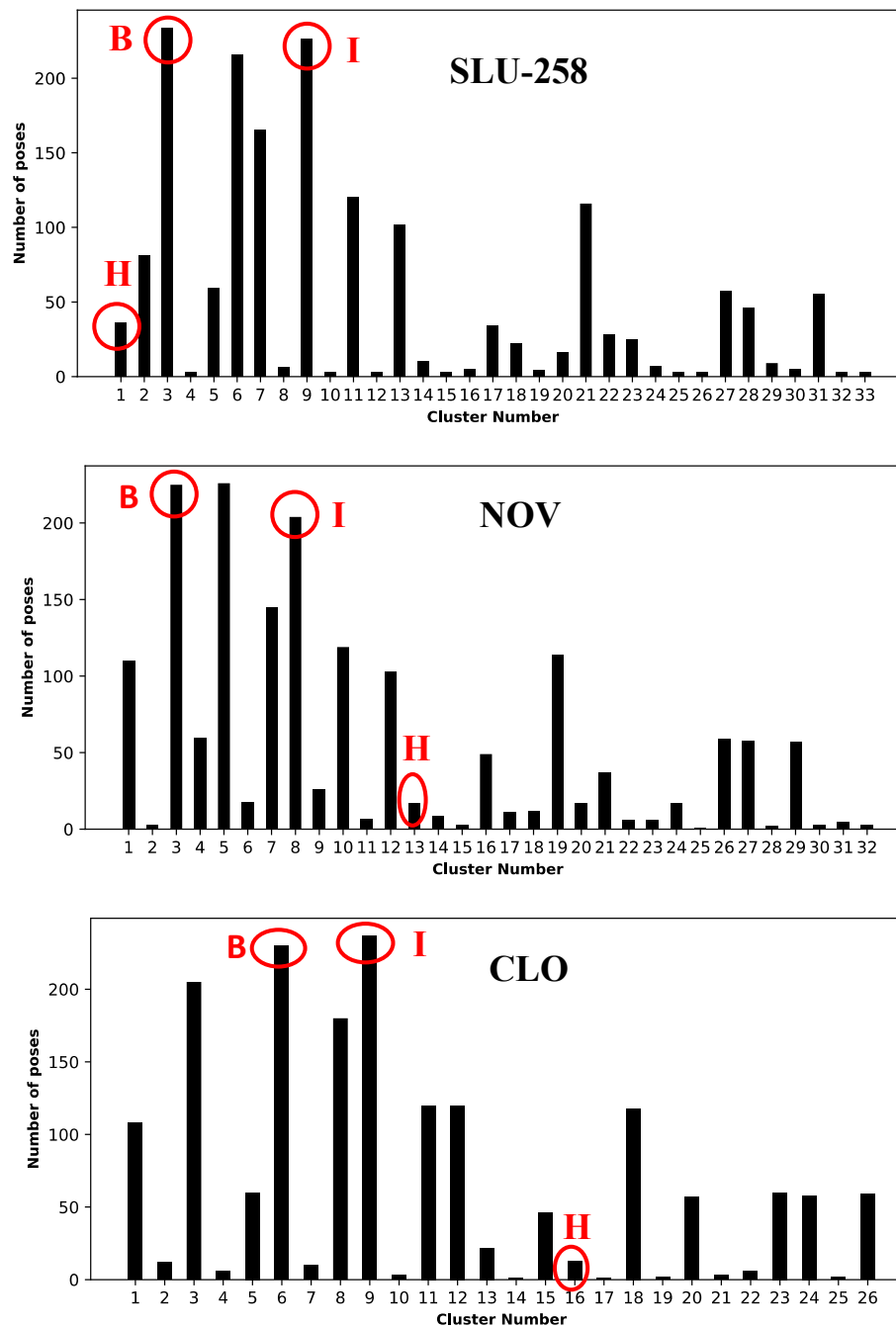


Figure S4. Number of occurrences of docked poses in each cluster determined from RMSD-based clustering of (A) SLU-258, (B) novobiocin, and (C) clorobiocin from blind ensemble docking. The three sites selected for MD simulation are circled in red and labeled as H (hinge), I (interfacial), and B (barrel). The RMSD cutoff was 2.5 Å.

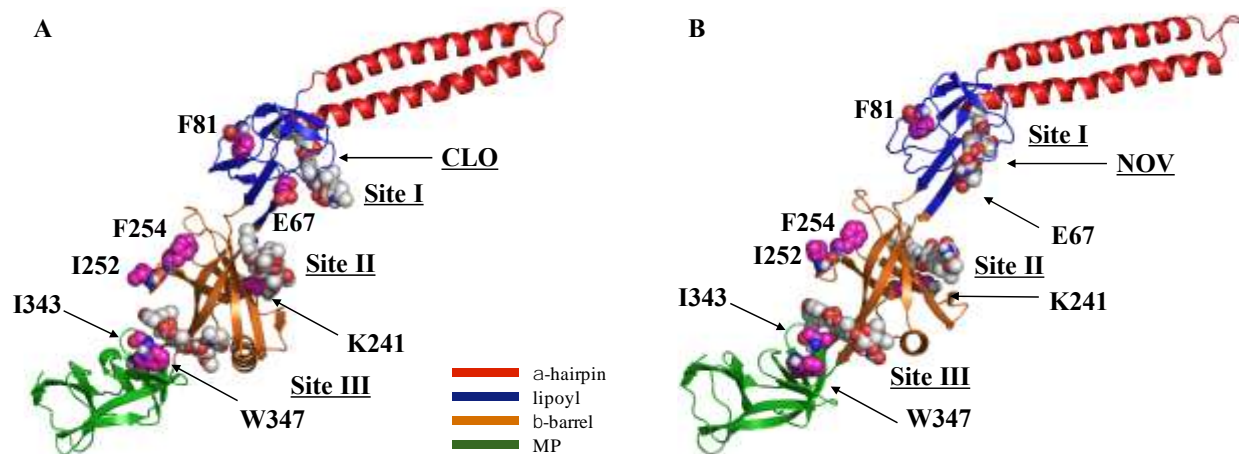


Figure S5. Three predicted sites from RMSD clustering of blind ensemble docking for (A) clorobiocin and (B) novobiocin referred to as the hinge, barrel, and interfacial sites. Residues mutated to Trp are E67, F81, I252, K241, F254, and I343. W347 was mutated to Phe.

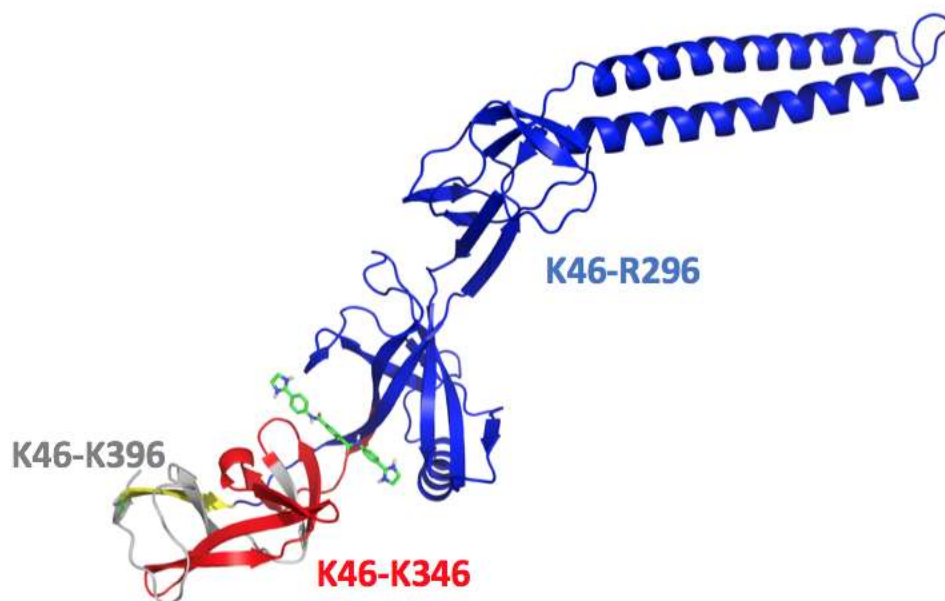


Figure S6. Predicted binding pose of SLU-258 (green sticks) at the interfacial site located between the β -barrel and MP domain. This site coincides with a previously observed proteolytic cleavage site of AcrA in the presence of SLU-258.¹⁰ The major fragment in the absence of inhibitor was K46-K346. However, two fragments, K46-R296 (blue) and K46-K346 (red plus blue), were observed in the presence of SLU-258. Residues 38-45, which were not included in the identification of the fragments, are shown in yellow.

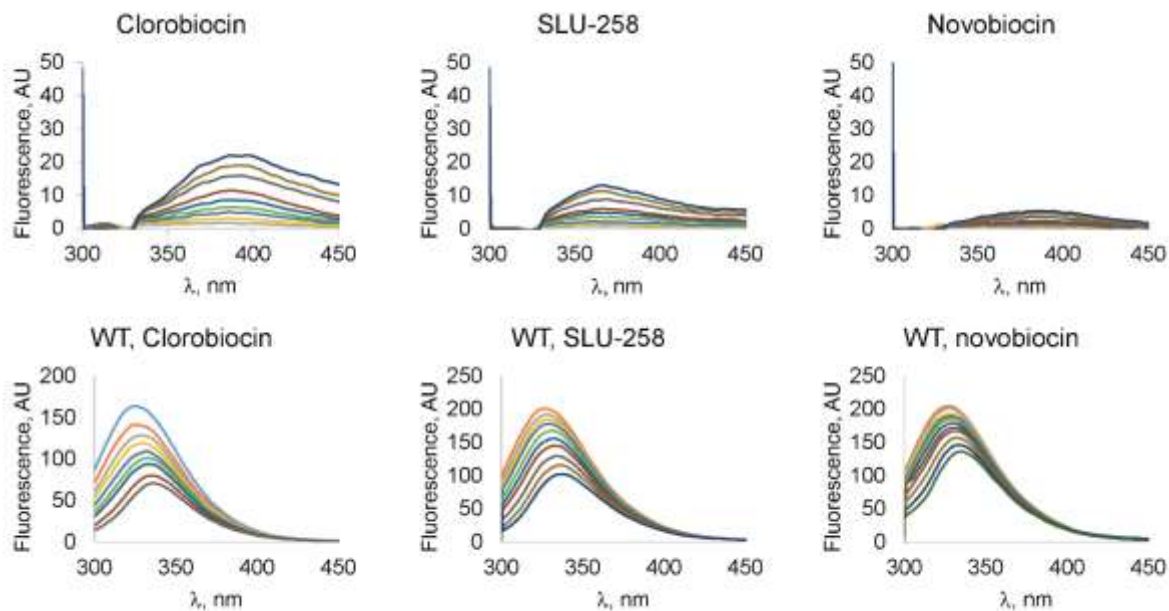


Figure S7. Fluorescence spectra of ligands and AcrA WT in the presence of increasing concentrations of inhibitors.

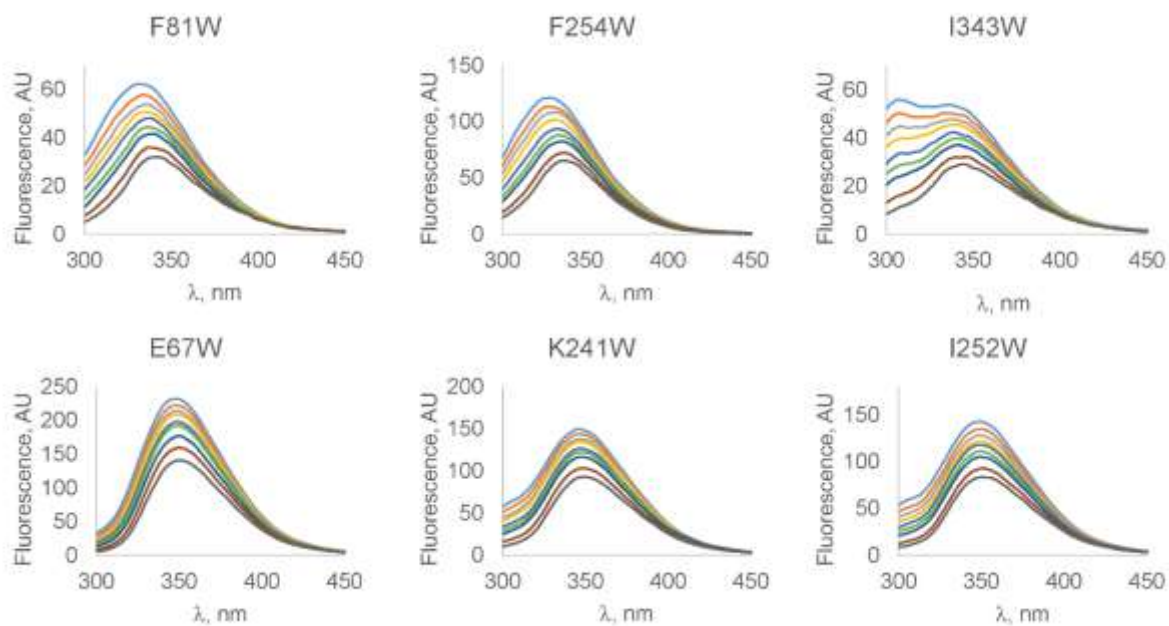


Figure S8. Fluorescence spectra of AcrA single Trp mutants in the presence of increasing concentrations of clorobiocin.

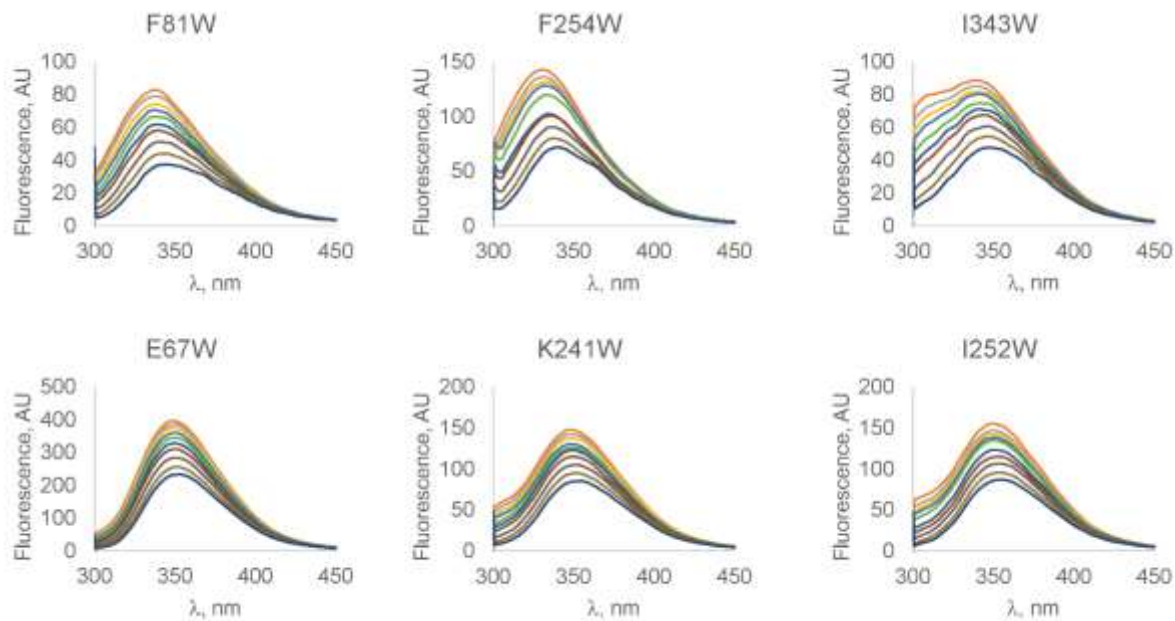


Figure S9. Fluorescence spectra of AcrA single Trp mutants in the presence of increasing concentrations of SLU-258.

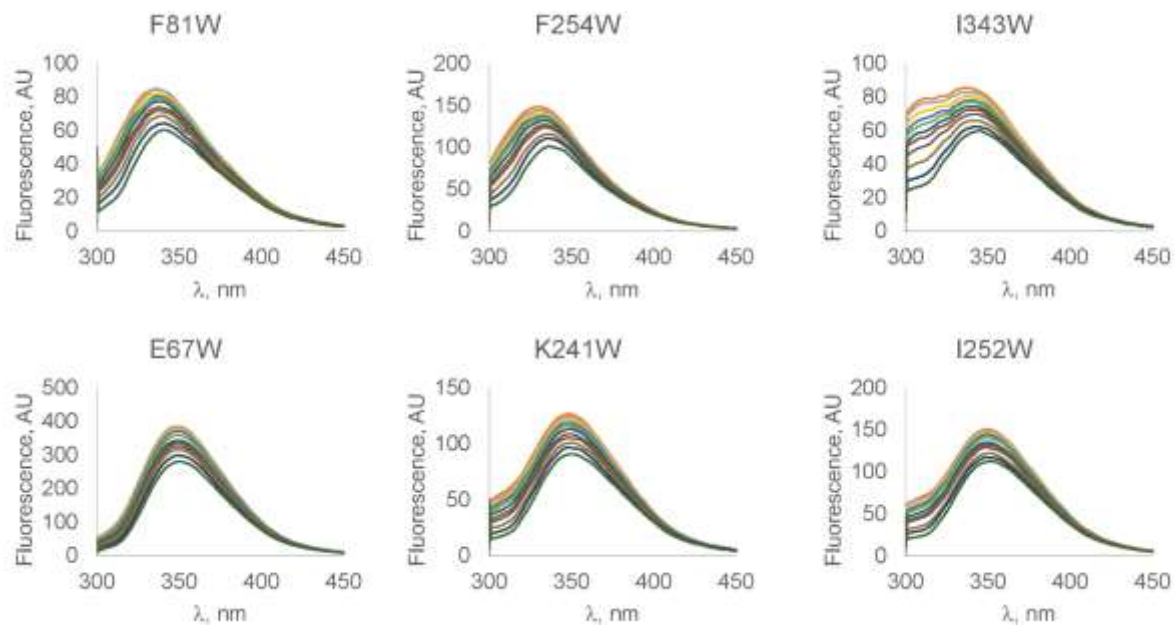


Figure S10. Fluorescence spectra of AcrA single Trp mutants in the presence of increasing concentrations of novobiocin.

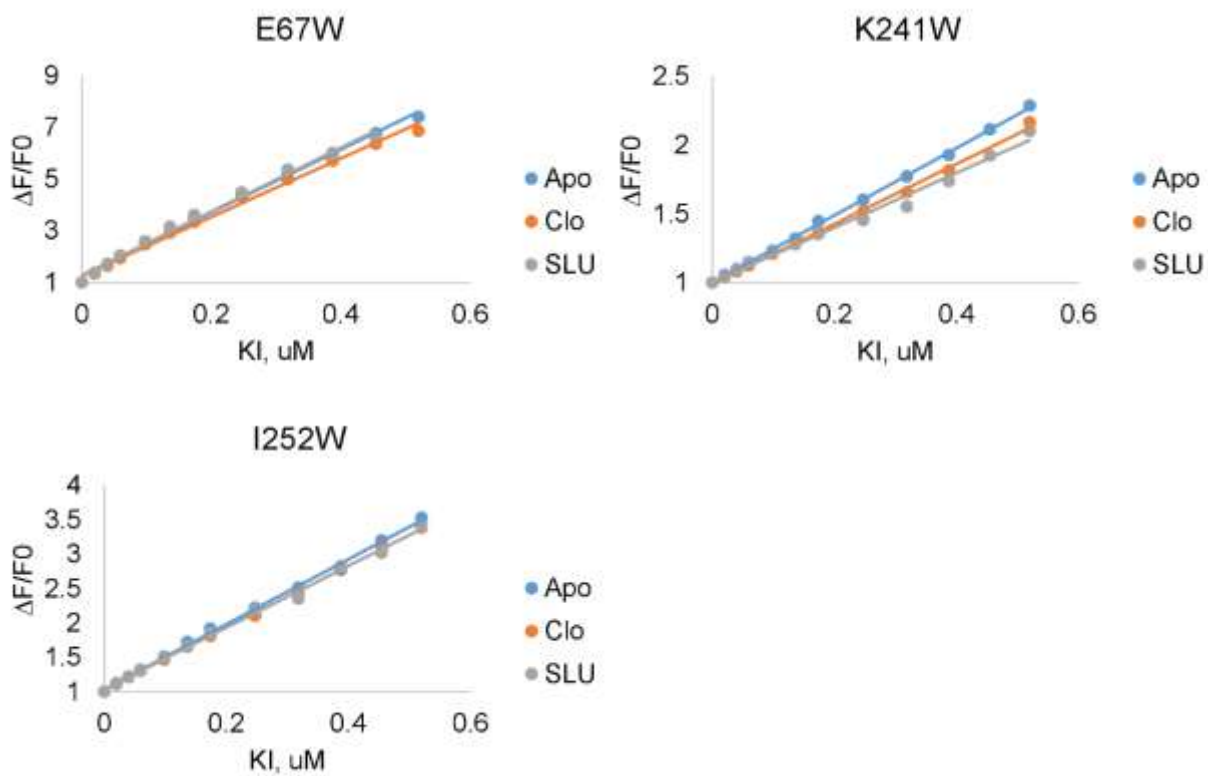


Figure S11. Trp fluorescence of E67W, K241W and I252W AcrA variants in the absence (Apo) and presence of clorobiocin (CLO) or SLU-258 (SLU) with increasing concentrations of potassium iodide (KI).